The HIAPER Cloud Radar Performance and Observations During Winter Storm Observations of a Nor'easter

S. Ellis[1*], R. Rauber[2], P. Tsai[1], J. Emmett[1], E. Loew[1], C. Burghart[1], M. Dixon[1], J. Vivekanandan[1], S. Rauenbuehler[1], J. Stith[1] and W-C. Lee[1]

1. National Center for Atmospheric Research, Boulder CO; 2. University of Illinois

1. HCR System Overview

The NCAR HIAPER Cloud Radar (HCR) is a W-band, airborne research radar developed to be housed in a standard large underwing aircraft pod as shown in Fig 1 (Vivekanandan et al., 2015). It is currently deployable on the NCAR GV HIAPER aircraft, but could theoretically be mounted on any aircraft that can accommodate a large pod and has the requisite wiring to run the radar.

Fig 1. Photo of the HCR pod mounted on the HIAPER aircraft's wing.

Within the pod a lens antenna illuminates a rotating reflector that allows the HCR to scan perpendicular to the aircraft (Fig. 2). The HCR can also operate in a staring configuration with active pointing stabilization to compensate the reflector angle to account for aircraft motion.

* *Corresponding author address:* Scott M. Ellis, National Center for Atmospheric Research, P.O. Box 3000, Boulder CO 80307; email: sellis@ucar.edu.

Many of the electronics are housed in the pressure vessel within the pod as shown in Fig. 2. The HCR uses one single rack inside the aircraft (Fig 2) thus saving valuable cabin space for additional instrumentation or seats.

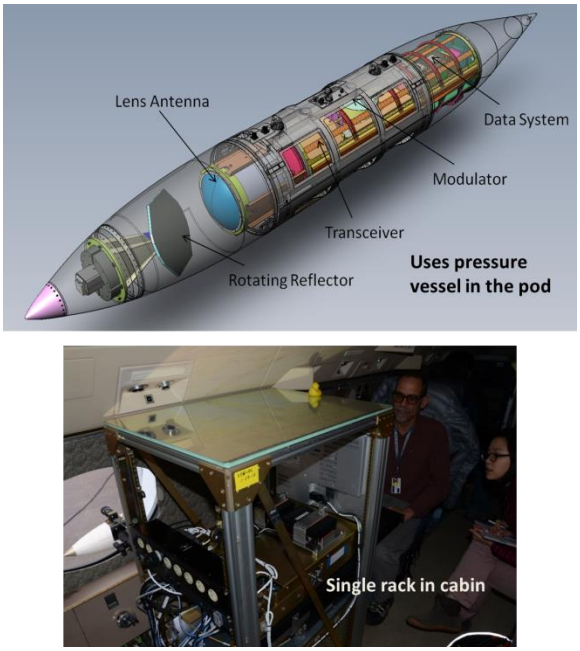

Fig. 2. The pressure vessel (above) and the cabin rack of the HCR (below).

The HCR is also deployable on the ground and is housed in half of a standard shipping container. The other half of the container contains the High Spectral Resolution Lidar (HSRL) enabling long-term zenith-pointing collocated radar and lidar measurements. This facilitates size estimates in liquid and ice.

The HCR is dual-polarimetric and Doppler capable. The most common configuration is to transmit in vertical polarization and receive both vertical and horizontal. This allows measuring the linear depolarization ratio (LDR), but not differential reflectivity. The measurements include: reflectivity (Ze), radial velocity (Vr), velocity spectrum width (SW) and LDR.

The range resolution of HCR can be selected from 20 to 150 m. The airborne beamwidth is 0.7 degrees and the ground-based is 0.25 degrees using a larger antenna. Nominally the along track resolution

is about 20 m. This is for 10 Hz data at 200 m s^{-1} ground speed.

The time series data are recorded for the HCR operations, enabling spectral analysis and techniques to be employed.

The specifications, design and capabilities of the HCR are described in more detail in Vivekanandan et al. (2015).

2. Navigation Correction

On a moving platform it is necessary to correct the radar pointing angle for the motion of the aircraft. With the groundspeed of the HIAPER exceeding 250 m s^{-1} at times, even small pointing errors can result in large Vr errors. The navigation correction requires accurate pointing and position data. The HCR has its own INS/GPS navigation system (CMIGITS II). The INS/GPS system is compact and is located near the reflector within the pod. It is important to have the INS/GPS in the pod since the motion of the pod may differ from that of the fuselage of the aircraft due to wing and pod flexing and vibrations. The navigation correction strategy of the HCR includes 2 steps; a real-time beam pointing stabilization and a final standard navigation correction based on measured pointing angles

The real-time stabilization updates the reflector position at a rate of 20 Hz based on the output of the INS/GPS system. The stabilization operates for staring mode data collection and keeps the beam very near the desired pointing angle. This is important to reduce the Vr errors from horizontal winds at non-flight levels being projected into the radial direction of off-nadir beams. This is illustrated in Fig. 3. It can be seen that for true nadir pointing there is no component of the horizontal wind along the radial. However if the beam is off-nadir the horizontal wind will project into the beam and contaminate the vertical Vr measurement. These errors can be corrected only if the vertical profile of the horizontal wind is known accurately, but this is often not the case.

The data are corrected using the final measured pointing angles following Lee et al. (1999). The corrections in this step are typically small if the beam pointing stabilization was active.

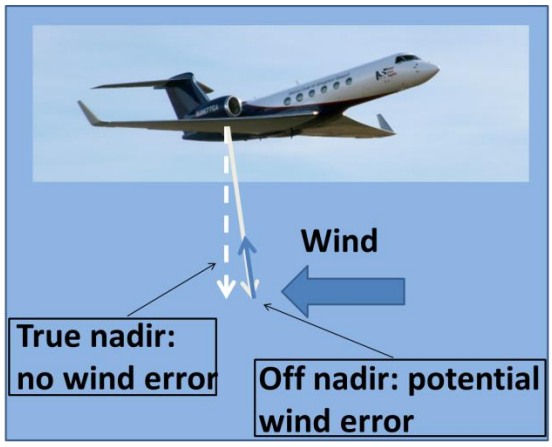

Fig. 3. Illustration of how the horizontal wind may be projected into the beam of off-nadir pointing radars.

3. Nor'easter: Rapid Response Project

The Nore'easter project was designed to study high impact winter storms in the northeast of the U.S. It was the first rapid-response deployment of an EOL facility. Prior to the deployment the HCR was mounted on the HIAPER aircraft and the aircraft was made ready to go from its base in Colorado. The Nor'easter PI's provided 5 day forecasts and outlooks with a 48 hour go/no-go decision requirement. Once the decision was made for the time period of the IOP (intensive operations period), the HIAPER was flown to a staging area in North Carolina on January 31st, 2015. The IOP was conducted on February 2nd 2015.

The sampling strategy was to fly transects along a set path between approximately Washington DC and Bangor Maine as drawn in the snowfall totals map of Fig. 3. The HIAPER aircraft made 3 round trips along the flight path for a total of 6 transects. From Fig. 3 it can be seen that the storm resulted in significant snowfall and the flight track was situated over some of the largest snow totals.

Fig. 4. A map of the NE U.S. showing the snow totals from the 2 February storm. The yellow line is the approximate location of the HIAPER flight track.

The HIAPER flew above the clouds at around 40 kft with the HCR staring at nadir. The active pointing stabilization was operating to keep the beam as close to nadir as possible. The HIAPER was on station from about 13:00 to 20:00 UTC.

4. Nor'easter Data Examples

The Nor'easter data set is largely of stratiform snow and rain. However the amount of fine-scale structure and detail is striking, including; cloud-top generating cells, upright elevated convection, layers of turbulence, complex structures across the melting level, gravity waves, boundary layer structures, and other complex features.

The detailed analysis of the observations is underway currently. In this section we present several data examples with interesting signatures in order to highlight the capabilities of the HCR radar and to document the complex and detailed structure of winter storms in the NE U.S. In the examples that follow, positive Vr is downward and negative Vr is upward motion, particle fall speed has not been removed, and the final aircraft navigation correction has been applied. All of the data examples shown will include 4 panels: upper left shows Ze, upper right shows Vr, lower left shows SW and lower right shows LDR.

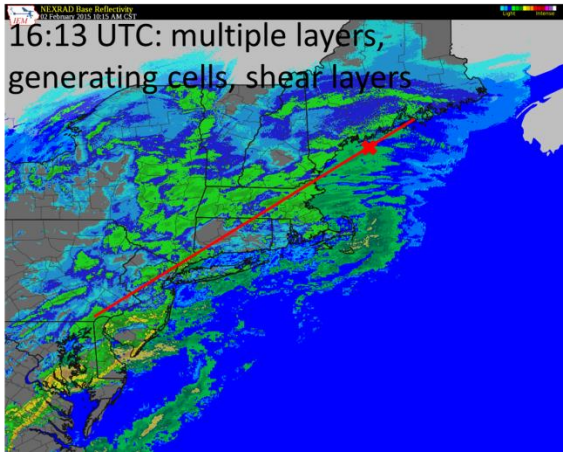

Fig. 5. Location of HCR for the data shown in Fig. 6.

The first example is from 16:13 UTC when the HCR was located over the ocean off the coast of Maine (Fig. 5). The WSR-88D composite in Fig. 5 shows light echoes of stratiform precipitation without many distinguishing features. Figure 6 shows one minute of data, or about 12 km distance, collected by HCR at this location. There is no evidence of a melting layer, which makes sense because the data were taken well north of the warm air of the system. Generating cells can be seen at the top of the echo at about 7 km height MSL. There are multiple layers of enhanced Ze and convective-looking updraft/downdraft pairs of various scales. Several shear layers are evident in the SW data.

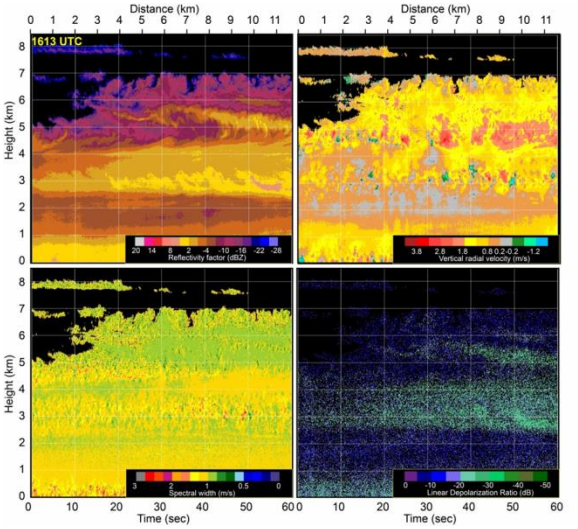

Fig. 6. Time/height plots of Ze, Vr, SW and LDR from 16:13 UTC.

The next example is located to the SW of the first over NE Massachusetts and is from 18:07 UTC. The WSR-88D radar composite shows very light stratiform echoes without noticeable structures.

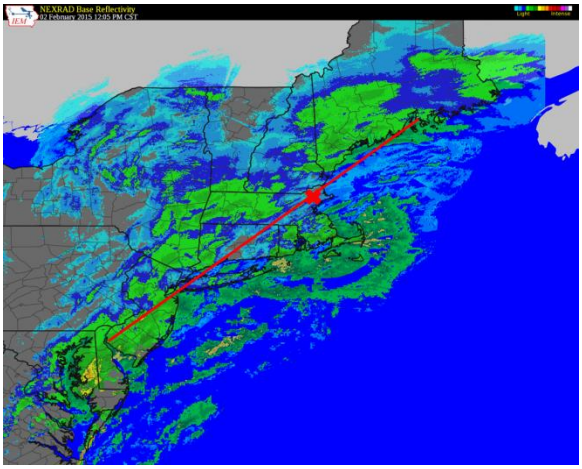

Fig. 7. Location of HCR for the data shown in Fig. 8.

The HCR detected waves at the top of the echo, which extends up to about 9 km. The waves have a wavelength of 4 to 5 km with updrafts and downdrafts as strong as 1.5 to 2 m s^{-1}. There are layers of enhanced Ze and shear layers evident in the SW.

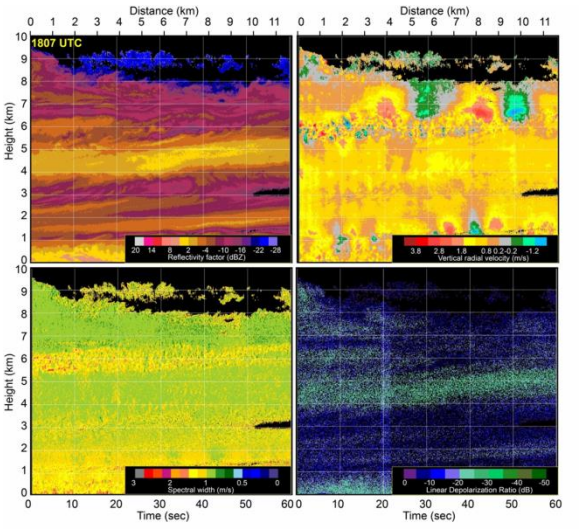

Fig. 8. Time/height plots of Ze, Vr, SW and LDR from 18:07 UTC.

The next example is from nearly the same location as the data shown in Fig. 8, but was about 3 hours earlier at 14:48 UTC (Fig. 9). The WSR-88D echo is stronger at this time and also stratiform in nature.

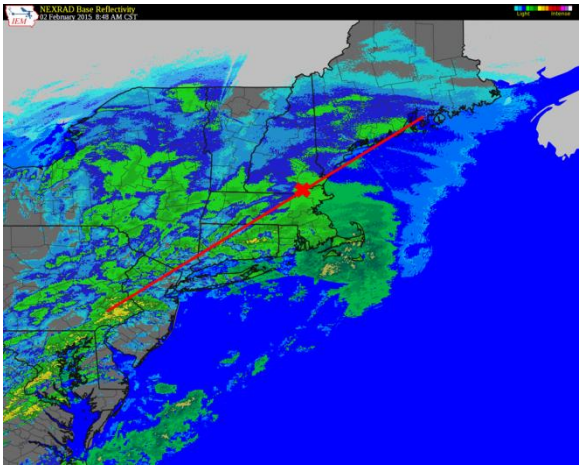

Fig. 9. Location of HCR for the data shown in Fig. 10.

Figure 10 shows one minute of HCR data from 14:48 UTC. There are multiple Ze layers with apparent connections. Small generating cells are evident at about 6 km and seem to be nearly de-coupled from the cloud layer below. The main stratiform echo is 3 to 4 km deep and contains strong wave structures in the Vr field. The up and downdrafts of these waves exceed 2 m s^{-1}. The waves are also evident as undulations in Ze, SW and LDR. Again there is no melting signature and the precipitation is frozen throughout.

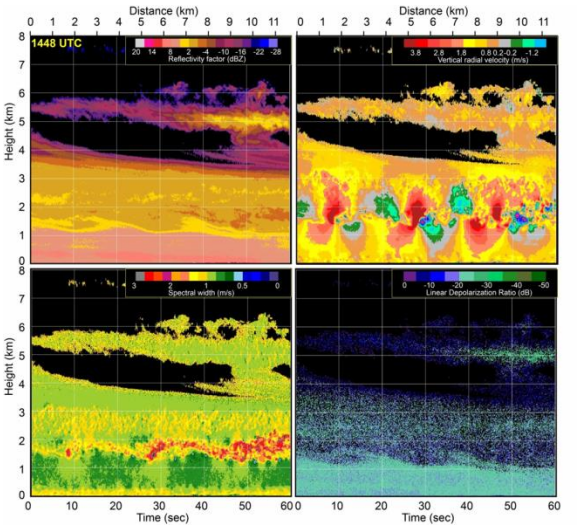

Fig. 10. Time/height plots of Ze, Vr, SW and LDR from 14:48 UTC.

The HIAPER continued its SW transect and about 15 minutes later at 15:03 UTC was in SW Connecticut as shown in Fig. 11. This was in the warm sector of the storm and the surface precipitation was rain. The WSR-88D showed light echoes with some smaller scale features and texture.

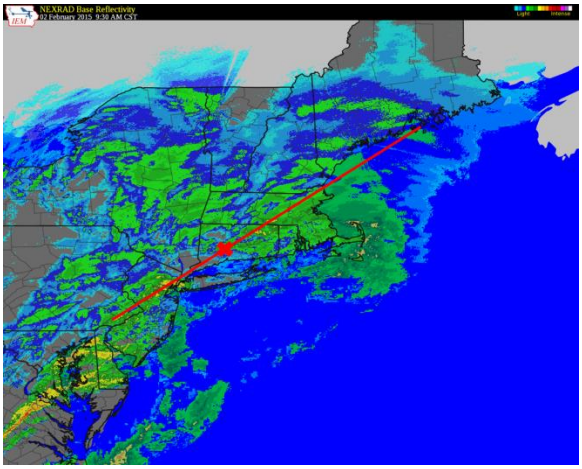

Fig. 11. Location of HCR for the data shown in Fig. 12.

Figure 12 shows the HCR data for one minute at 15:03 UTC. There are wave-like structures evident in the Vr field with up and downdrafts in excess of 1 m s^{-1} at about 5 km height. These seem to be associated with fall streaks in the Ze field. There are larger wavelength waves in the middle part of the echo with a wavelength of about 6 km (the minute of data is about 12 km). These waves are also deeper in extent. There is a pronounced melting layer signature around 1.5 km height. The melting level is evident by increased Ze and a layer of increased LDR. The Vr in

the rain is higher than in the snow as can be seen by the larger Vr values below the melting layer. Also the SW is higher in the rain because different sizes of raindrops have more variation in terminal fall speed than ice. There are many undulations in the melting level apparent in the LDR field.

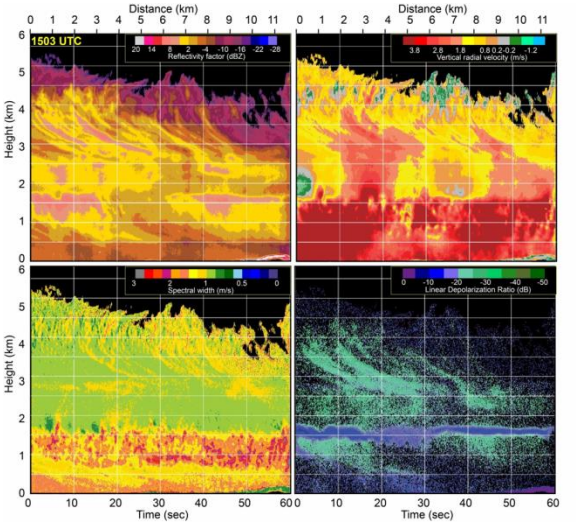

Fig. 12. Time/height plots of Ze, Vr, SW and LDR from 15:03 UTC.

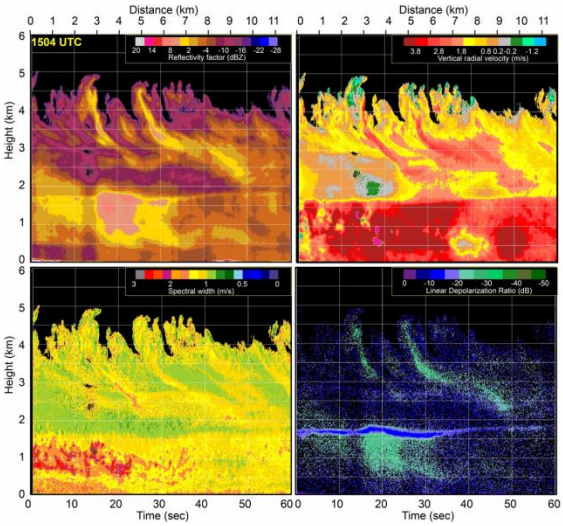

Fig. 13. Time/height plots of Ze, Vr, SW and LDR from 15:04 UTC.

The rapid change in the character of the data is striking. As an example, Fig. 13 shows data from the next minute of flight as shown Fig 12, beginning at 15:04 UTC. The data from 15:04 has different scales of circulations and looks remarkably different than the data at 15:03 UTC. The generating cells apparent between 4 and 5 km height have updraft speeds exceeding 1 m s^{-1} (not accounting for fall speed). There are notable fall streaks in the Ze field associated with the generating cells.

6. Summary and Conclusions

The HCR made its maiden scientific mission during Nor'easter, the first rapid-response project for an EOL platform. The HCR performed quite well and documented numerous fine-scale features that are not detected by the ground-based radar network. The rapid-response framework was very successful. The data collected during Nor'easter is a fascinating collection of cloud-top generating cells, upright elevated convection, layers of turbulence, complex structures across the melting level, gravity waves, boundary layer structures, and other complex and mysterious features. It is felt that the Nor'easter data set will provide scientific investigations and insights long into the future.

Acknowledgments

The National Center for Atmospheric Research is sponsored by the National Science Foundation. Any opinions, findings and conclusions or recommendations expressed in this publication are those of the author(s) and do not necessarily reflect the views of the National Science Foundation.

7. References

Lee, W. C., Dodge, P., Marks, F. D., and Hildebrand, P. H.: Mapping of airborne Doppler radar data, J. Atmos. Ocean. Tech., 11, 572–578, 1994.

Vivekanandan, J., S. M. Ellis, P. Tsai, E. Loew, W.-C. Lee, J. Emmett, M. Dixon, C. Burghart and S. Rauenbuehler, 2015: A wing pod-based millimeter wavelength airborne cloud radar, *Geosci. Instrum. Method. Data Syst.*, **4**, 161-176, doi:10.5194/gi-4-161-2015.